Asymmetric Hydrogenation

DOI: 10.1002/ange.201006870

Enhancement of the Performance of a Platinum Nanocatalyst Confined within Carbon Nanotubes for Asymmetric Hydrogenation**

*Zhijian Chen, Zaihong Guan, Mingrun Li, Qihua Yang, and Can Li**

The technology for generating chiral molecules plays increasingly important roles in drug research.[1–2] Though numerous highly efficient homogeneous asymmetric catalysts have been developed for the synthesis of chiral molecules in the past decades,[3–8] only limited numbers of them have been used in industry because of the intrinsic problems of homogeneous asymmetric catalysis, such as difficulty in product separation and purification, and recycling of the catalysts. Fortunately, heterogeneous asymmetric catalysis can overcome these problems and has thus become one of the most desirable approaches for the large-scale production of chiral compounds.[9–14] However, most heterogeneous chiral catalysts are often plagued by low activity or poor enantioselectivity, which impedes the practical applications of heterogeneous asymmetric catalysis.[15,16] The modification of active metal surfaces, to create a chiral microenvironment through adsorption of chiral molecules has proven to be an efficient strategy for developing heterogeneous chiral catalysts.[17–19] Chirally modified Raney Ni, Pt, and Pd catalysts represent successful examples of this strategy.[20–23] For years, extensive efforts have been made for the development of more advanced chirally modified heterogeneous catalysts,[18] including exploration of active metals, changing the properties of the supports, employing various kinds of chiral modifiers, and screening suitable substrates.[24–26] However, the attempts to additionally increase the activity and enantioselectivity of the heterogeneous chiral catalysts seems less successful.

Carbon nanotubes (CNTs) are attractive materials as supports or catalysts. As a result of the possible confinement effect of CNTs, employment of the CNTs channels as nanoreactors for asymmetric catalysis may provide opportunities for the development of new heterogeneous chiral catalysts. However, the applications of CNT channels in asymmetric catalysis have not been reported, as far as we know.

Herein we report the asymmetric hydrogenation reactions using chirally modified Pt nanoparticles encapsulated within CNT channels. The activity and enantioselectivity of a Pt nanocatalyst confined inside the CNT nanochannels (denoted as Pt/CNTs(in); Scheme 1), are greatly enhanced for the asymmetric hydrogenation of α-ketoesters using cinchonidine (CD) as the chiral modifier. The average turnover frequency

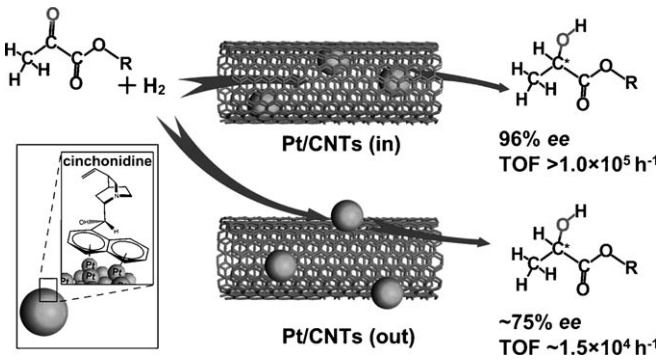

Scheme 1. Asymmetric hydrogenation of α-ketoesters on the Pt nanoparticles encapsulated within the CNTs (Pt/CNTs(in)) and adsorbed onto CNTs (Pt/CNTs(out)) with cinchonidine (CD) as a chiral modifier.

(TOF) achieved on Pt/CNTs(in) is above $1.0 \times 10^5\ h^{-1}$, which is amongst the highest TOF ever reported for heterogeneous asymmetric hydrogenations;[18,22,24,27] this TOF is even much higher than that of Pt nanocatalysts loaded onto the outer surface of CNTs [denoted as Pt/CNTs(out)]. The transmission electron microscopy (TEM) analysis and adsorption and kinetic studies reveal that the high activity and enantioselectivity of the CNT-encapsulated Pt nanoparticles are associated with the ultrahigh enrichment of the chiral modifier and reactants inside the channels of the CNTs. These results show the important and unique features of the asymmetric catalysis within the nanotubes, and that the nanochannels of CNTs act as highly efficient nanoreactors for the heterogeneous asymmetric hydrogenations.

The CNTs used in this work were shortened, functionalized, and then the ends were opened (see Figure S1 in the Supporting Information). Pt/CNTs(in) catalysts were prepared by encapsulating 5 wt% Pt within the channels of multiwalled CNTs, and Pt/CNTs(out) catalysts were prepared by depositing 5 wt% Pt on the outer surface of the multiwalled CNT channels. A commercial 5 wt% Pt/AC (AC = activated carbon) catalyst was used for comparison. The surface-area data of the catalysts and carbon nanotube materials are given in Table S1 in the Supporting Information. Pt/CNTs(in) and Pt/CNTs(out) have the same BET surface area of 201 $m^2 g^{-1}$. Pt/AC (BET surface area of 930 $m^2 g^{-1}$) has a much higher surface area than those of Pt/CNTs(in) and Pt/

[*] Dr. Z. J. Chen, Z. H. Guan, Prof. M. R. Li, Prof. Q. H. Yang, Prof. C. Li
State Key Laboratory of Catalysis, Dalian Institute of Chemical Physics, Chinese Academy of Sciences
457 Zhongshan Road, Dalian 116023 (China)
E-mail: canli@dicp.ac.cn

[**] This work was financially supported by the Natural Science Foundation of China (NSFC 20773123 and NSFC 20621063) and the National Basic Research Program of China (2010CB833300). We thank Hongxian Han and Fengtao Fan for revision of the manuscript, and Yan Liu, Qiang Gao, Jun Li, and Xiaohong Li for helpful discussions.

Supporting information for this article is available on the WWW under http://dx.doi.org/10.1002/anie.201006870.

CNTs(out). The location and particle size of Pt were characterized by TEM analysis. The TEM images of Pt/CNTs(in) show that most of the platinum nanoparticles are evenly distributed within the CNT nanochannels (Figure 1a; Figures S3–S4 and S22). The location of the Pt nanoparticles within the nanochannels of the CNTs of the Pt/CNTs(in) catalyst was additionally confirmed by the TEM images of the Pt nanoparticles recorded at different tilting angles (Figures S2 and S3). The TEM images of Pt/CNTs(out) clearly show that the Pt nanoparticles are dispersed on the outer surface of the CNTs (Figure 1b; Figure S4). The particle sizes of Pt in Pt/CNTs(in) and Pt/CNTs(out) are estimated to be approximately 3.5 nm from the TEM images (Figure 1; Figure S4); and the particle sizes of Pt in Pt/CNTs(in) and Pt/CNTs(out) are about 3.4 and 3.7 nm, respectively, as determined by CO chemisorption (Table S2). However, the Pt/AC catalyst has randomly distributed Pt nanoparticles and the particle sizes range from 1.0 to 9.0 nm with an average particle size of 4.6 nm (Figure 1).

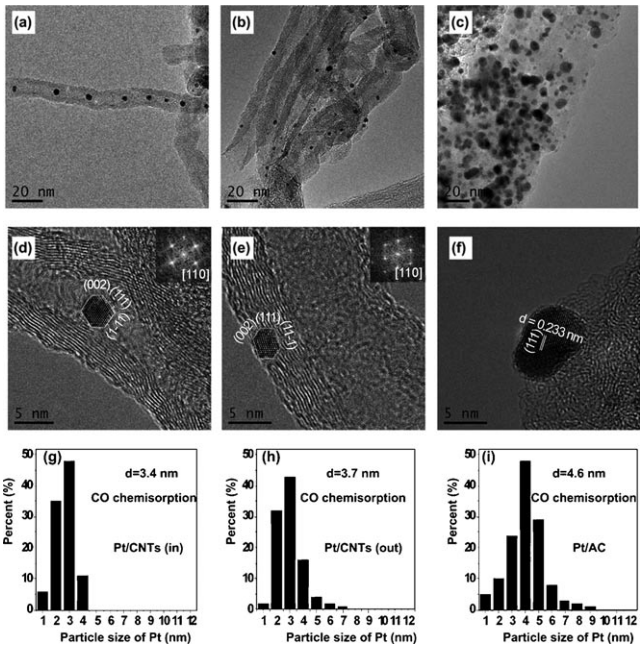

Figure 1. TEM images of catalysts and the platinum particle size distribution. Low-magnification TEM images of a) Pt/CNTs(in), b) Pt/CNTs(out), and c) Pt/AC. HRTEM images of d) Pt/CNTs(in) viewed along [110] direction, e) Pt/CNTs(out) viewed along [110] direction, and f) Pt/AC catalyst. The platinum particle-size distribution is based on TEM characterization and the average particle size estimate is based on CO chemisorption for g) Pt/CNTs(in), h) Pt/CNTs(out), and i) Pt/AC.

Table 1 lists the catalytic performances of Pt/CNTs(in), Pt/CNTs(out), and Pt/AC (Pt loading for all catalysts is 5 wt%) in the asymmetric hydrogenation of α-ketoesters using cinchonidine (CD) as the chiral modifier. For the asymmetric hydrogenation of ethyl pyruvate (ETP; a representative substrate), the CNTs (with open ends) show no catalytic activity and enantioselectivity (Figure 2). Pt/CNTs(in), Pt/CNTs(out), Pt/AC, and Pt/Al_2O_3 have TOF values of $1.0\times10^5\ h^{-1}$, $1.5\times10^4\ h^{-1}$, $7.0\times10^3\ h^{-1}$, and $1.0\times10^4\ h^{-1}$, respectively. The catalytic activity of Pt/CNTs(in) is extremely high and even superior to that of the well-known Pt/Al_2O_3 catalyst under the same reaction conditions. It is also noteworthy that not only the activity is significantly high but also the enantioselectivity; Pt/CNTs(in) delivers products with 96% *ee*, which is higher that of Pt/CNTs(out) (75% *ee*), Pt/AC (61% *ee*), and Pt/Al_2O_3 (90% *ee*). For the substrates methyl pyruvate (MEPY) and ethyl 2-oxo-4-phenyl-butyrate (EOPB), the Pt/CNTs(in) achieves 96% *ee* with a TOF of over $1.2\times10^5\ h^{-1}$, and 86% *ee* with a TOF of over $2.0\times10^4\ h^{-1}$, respectively. These catalysts exhibit similar trends in activity and enantioselectivity, namely, Pt/CNTs(in) shows

Table 1: Asymmetric hydrogenation of α-ketoesters on different catalysts modified with cinchonidine (CD).[a]

Substrate	Catalyst	TOF [h^{-1}]	*ee* [%]
ETPY	Pt/CNTs(in)	>100000	96
	Pt/CNTs(out)	15000	75
	Pt/CNTs(in) (without CD)	4680	racemic
	Pt/CNTs(out) (without CD)	682	racemic
	Pt/AC	7000	61
	Pt/Al_2O_3	10330	90
MEPY	Pt/CNTs(in)	>120000	96
	Pt/CNTs(out)	16500	76
	Pt/AC	7500	63
	Pt/Al_2O_3	11500	91
EOPB	Pt/CNTs(in)	>20000	86
	Pt/CNTs(out)	1460	58
	Pt/AC	900	35
	Pt/Al_2O_3	1600	83

[a] Pt loading for all catalysts is 5 wt%. The molar ratio for CD/Pt is within the range of 8.0–10.5 for all the reactions. Reaction conditions: 20 mg of catalyst, 4.0 mg of cinchonidine (1.345×10^{-2} mmol), 0.20 mL of substrates, 4 mL of acetic acid, H_2 pressure of 6.0 MPa, 293 K (for details see the Supporting Information S1.3).

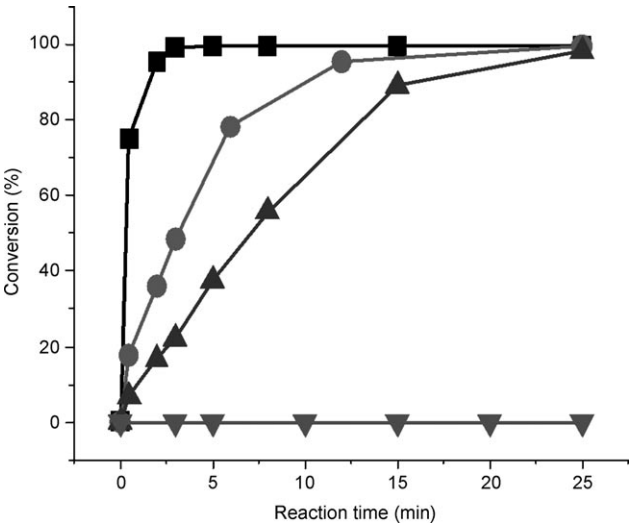

Figure 2. The asymmetric hydrogenation of ETPY on Pt/CNTs(in) (■), Pt/CNTs(out) (●), commercial Pt/AC (▲), and opened CNTs (▼) as a function of reaction time. Reaction conditions are the same as those used in Table 1 (for details see the Supporting Information S1.3).

much higher activity and enantioselectivity than Pt/CNTs-(out) and Pt/AC. The enantioselectivity for all the substrates follows the order of Pt/CNTs(in) > Pt/CNTs(out) > Pt/AC.

In the absence of CD, Pt/CNTs(in) and Pt/CNTs(out) can also catalyze the hydrogenation of ETPY to produce racemic products. Pt/CNTs(in) shows a TOF of over 4600 h^{-1}, which is much higher than that of 680 h^{-1} for Pt/CNTs(out). It is evident that Pt particles encapsulated within the nanochannels of CNTs show much higher hydrogenation activity than that of Pt particles located on the outer surface of CNTs. The TOFs of Pt/CNTs(in) and Pt/CNTs(out) without CD are obviously lower than those with CD, confirming the acceleration effect[27] of the chiral ligand for the asymmetric hydrogenation of α-ketoesters in CNTs. The TOFs of Pt/CNTs(in) and Pt/CNTs(out) are accelerated up to over 20 times in the presence of CD (Table 1).

Figure 2 presents the kinetic behavior of the asymmetric hydrogenation of ETPY using Pt/CNTs(in), Pt/CNTs(out), and Pt/AC catalysts. The reactant conversion can be 100% in about 2 minutes for Pt/CNTs(in), whereas it takes over 15 minutes for Pt/CNTs(out) and 25 minutes for Pt/AC. The Pt/CNTs(in) catalyst shows extremely high initial activity and as high as 80% of the conversion can be obtained in less than 1 minute. The Pt/CNTs(out) catalyst achieves only less than 30% conversion, and even less for the Pt/AC catalyst. It is amazing that the asymmetric hydrogenation reaction in Pt/CNTs(in) is so fast that the reactant can be converted into the product in a few minutes within the carbon nanotubes having a diameter of only 8–10 nm; additionally, the enantioselectivity of Pt/CNTs(in) is always higher than that of Pt/CNTs(out) for different types of reactants.

The mechanism of asymmetric catalysis on chirally modified metal surfaces is complicated and is not yet been well understood. It is generally believed that the chiral modifier CD that is adsorbed onto Pt surface not only induces the enantioselectivity of the reaction, but also accelerates the reaction rate of Pt catalysts for the asymmetric hydrogenation of α-ketoesters.[23,27] To study the influence of CD on the catalytic performance of Pt/CNTs(in) and Pt/CNTs(out), the asymmetric hydrogenation of ETPY was performed at different CD concentrations. The CD concentration was varied within the range of $3.4–85.0\times10^{-4}$ mol L^{-1}, and both the enantioselectivity and TOF of Pt/CNTs(in) remain almost the same (Figures S8 and S9); Pt/CNTs(out) shows a similar tendency. This result suggests that a small change in the CD concentration under the current catalytic conditions (CD concentration, 34.0×10^{-4} mol L^{-1}) has nearly no influence on the enantioselectivity and catalytic activity for both Pt/CNTs(in) and Pt/CNTs(out). Therefore, we conclude that the difference in enantioselectivity between Pt/CNTs(in) and Pt/CNTs(out) may not be due to the small variation of the CD concentration in solution during the catalytic process.

The different types of crystal planes for metal particles generally have big influence on the catalytic performance.[28,29] To clarify the effect of the morphology of the Pt nanoparticles on catalytic performance, the crystallographic nature of the individual Pt nanoparticles of Pt/CNTs(in) and Pt/CNTs(out) was examined by high-resolution transmission electron microscopy (HRTEM; Figures S5 and S6), the results of which show that the Pt nanoparticles that are either inside or outside the CNT have similar morphologies. On the basis of the HRTEM images observed along the [100] and [110] directions, the three-dimensional crystal shapes of the Pt nanoparticles in both the Pt/CNTs(in) and Pt/CNTs-(out) catalysts were reconstructed (Figure S6), and the crystal exposes its eight {111} planes and six {100} planes. The summed Pt {111} area is estimated to be 85% of the total area. Baiker et al. reported that the good enantioselectivity for hydrogenation on Pt/Al_2O_3 (5 wt% Pt) might partially be attributed to the high exposure ratio of the Pt {111} planes.[30] The results of TEM analysis clearly show that the size and the morphology of the Pt nanoparticles for both Pt/CNTs(in) and Pt/CNTs(out) are almost the same. Therefore, in this work, the significant difference in catalytic performance including the activity and the enantioselectivity of Pt/CNTs(in) and Pt/CNTs(out) seems to not be due to the morphology and particle size of Pt nanoparticles that reside either inside or outside CNTs nanochannels.

Figure 3 shows the adsorption of CD by each of the catalysts and the closed CNTs (for the adsorption details see the Supporting Information S1.4 and Figures S10–15). To exclude the factor of the surface area, the adsorption uptake was normalized by BET surface area of the adsorbents (Figure 3). Pt/CNTs(in) shows the highest adsorption concentration of CD among the catalysts. Pt/CNTs(out) exhibits a slightly lower adsorption concentration of CD than Pt/CNTs(in), but it is much higher than that of the closed CNTs. With Pt/AC having the highest BET surface area, it shows the lowest CD adsorption concentration. The closed CNTs adsorb only less than 10% CD from the initial solution after 25 minutes (Figure S15). However, Pt/CNTs(in) and Pt/CNTs(out) show fast adsorption kinetics by taking 80% CD from solution in less than 2 minutes (Figure S15), and the open CNTs exhibit similar adsorption kinetics by taking

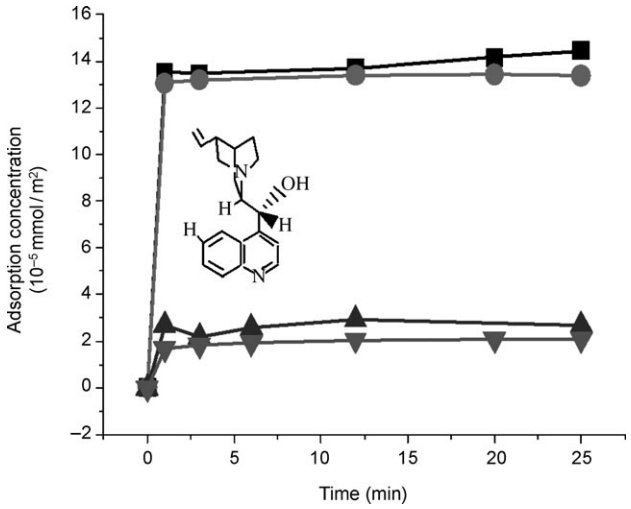

Figure 3. Comparison of the concentration of the adsorbed CD, normalized by BET surface area of adsorbents as a function of adsorption time, for Pt/CNTs(in) (■), Pt/CNTs(out) (●), commercial Pt/AC (▼), and closed CNTs (▲).

about 80% CD from solution after 3 minutes (Figure S14). Based on the adsorption data, the CD concentration in the channels of Pt/CNTs(in) is about 2700 times higher than that in solution (for calculation details see the Supporting Information S1.4). This data suggests that the CD can be enriched in the channels of CNTs irrespective of the location of Pt particles inside or outside of the CNT channels. Pt/AC can also adsorb CD (Figures S13 and S15), but the amount of CD adsorbed is much less than that of Pt/CNTs(in) and Pt/CNTs(out).

Figure 4A shows the adsorption concentration of ETPY (reactant) onto the Pt/CNTs(in), Pt/CNTs(out), and Pt/AC catalysts. The adsorption of ETPY onto Pt/CNTs(in) and Pt/CNTs(out) is very fast and the adsorption equilibrium was

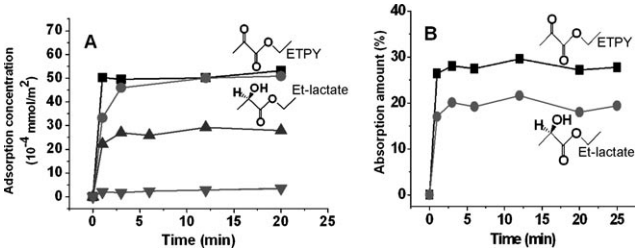

Figure 4. Adsorption kinetics of the reactant (ETPY) and product ((*R*)-ethyl lactate). A) Comparison of ETPY adsorption concentration as a function of time on Pt/CNTs(in) (■), Pt/CNTs(out) (●), and commercial Pt/AC (▼). The adsorption concentration of (*R*)-ethyl lactate as a function of time on the Pt/CNTs(in) (▲)catalyst. B) Co-adsorption of a mixture of ETPY (■) and (*R*)-ethyl lactate (●; the mole ratio of ETPY/(*R*)-Et-lactate = 1.1) as a function of time on Pt/CNTs(in). The adsorption amount was calculated based on GC analysis.

achieved in less than 3 minutes; more than 35% ETPY in the solution can be adsorbed (Figures S16–S21). However, Pt/AC shows an obviously lower adsorption concentration and less than 15% ETPY from the solution is adsorbed. The ETPY concentration in the channels of CNTs is about 400 times higher than ETPY in solution based on the adsorption data (see the Supporting Information S1.4). This result shows that the reactant can be also enriched in the channels of CNTs.

The adsorption concentration of CD or ETPY for Pt/AC is much lower than that of Pt/CNTs(in) or Pt/CNTs(out) as shown in Figures 3 and 4A. These data indicates that the capillary adsorption effect of the opened nanochannels of CNTs has a vital impact on the adsorption uptake. The adsorption results suggest that open CNT channels have a unique enrichment effect on both CD and the reactant, ETPY, and is probably due to the intensified capillary effect of CNT channels when their diameters are in the nanoscale range. Therefore, the ultrahigh enrichment of both CD and ETPY in CNT channels is proposed to be a reason for the dramatically different catalytic performances of Pt/CNTs(in) and Pt/CNTs(out). The channels of the CNTs with ultrahigh enrichment of CD should favor the strong and high density adsorptions of CD and ETPY on Pt nanoparticles inside the channels of CNTs, thus contributing to the higher reaction rate and enantioselectivity of Pt/CNTs(in) relative to those of Pt/CNTs(out).

Figure 4B gives the competitive adsorption of the reactant, ETPY, and the hydrogenation product, (*R*)-Et-lactate by Pt/CNTs(in). Both the reactant and the product are adsorbed very quickly, and reach the adsorption equilibrium in a few minutes. However, the equilibrium amount of the reactant adsorbed is about 40–50% higher than that of product adsorbed within Pt/CNTs(in). These facts indicate that the channels of CNTs have the ability to discriminate between the reactants and products having slightly different hydrophilicity/hydrophobicity. As a result, the CNT channels are kinetically favorable for the asymmetric hydrogenation of α-ketoesters.

To evaluate the stability of the catalyst, the recycling of Pt/CNTs(in) was performed for the asymmetric hydrogenation of ETPY. The solid catalyst was recovered by centrifugation (or filtration), washed with acetic acid in air, and re-modified by CD in acetic acid. A constant conversion of 99.9% with up to 96% enantioselectivity was obtained even after nine consecutive cycles of the reaction. The result indicates that the Pt/CNTs(in) catalyst is quite stable and can be recycled without deterioration in activity or enantioselectivity (Table S3).

In summary, we found that when a Pt nanocatalyst modified by CD was encapsulated within CNTs it is very active and leads to the highly enantioselective hydrogenation of α-ketoesters. The high activity and enantioselectivity are attributed mainly to the unique properties of the nanochannels of the CNTs as they can readily enrich both CD and the reactants. This work shows the unique effect of the nanochannels of CNTs as nanoreactors for asymmetric catalysis. The encapsulation of a nanocatalyst and chiral modifier within CNTs as described in this work opens an opportunity for developing novel, highly active and enantioselective heterogeneous chiral catalysts.

Experimental Section

Preparation of Pt/CNTs(in) and Pt/CNTs(out): The Pt/CNTs(in) catalyst was prepared by introducing the platinum precursor (5% wt) into the CNTs channels using an improved wet-chemistry method.[31,32] The CNTs (2.0 g) with open ends (for the preparation see the Supporting Information S1.2) were immersed in an aqueous solution of H_2PtCl_6 (50 mL, 10.25 mmol L^{-1}) at room temperature. After ultrasonic treatment for 3 h, the mixture was stirred for 48 h at room temperature. Then the mixture was heated to 110 °C with a heating rate of 1 °C min^{-1} and held at 110 °C for 24 h. By this slow drying method, the catalyst precursor was introduced into the CNTs channels. The dried sample was reduced with a sodium formate solution (42 mg mL^{-1}) at 100 °C for 1 h, and then the solid product was filtered, washed with deionized water, and dried at 60 °C for 18 h. The process for the synthesis of Pt/CNTs(out) was described in the Supporting Information. For the TEM characterization and asymmetric hydrogenation see the Supporting Information.

Received: November 2, 2010
Revised: January 25, 2011
Published online: March 2, 2011

Keywords: asymmetric hydrogenation · carbon nanotubes · heterogeneous catalysis · nanoparticles

[1] A. M. Rouhi, *Chem. Eng. News* **2003**, *81(18)*, 45 – 55.
[2] A. M. Rouhi, *Chem. Eng. News* **2004**, *82(24)*, 47 – 62.
[3] E. N. Jacobsen, A. Pfaltz, H. Yamamoto in *Comprehensive Asymmetric Catalysis*, Springer, Berlin, **1999**.
[4] M. S. Taylor, E. N. Jacobsen, *Proc. Natl. Acad. Sci. USA* **2004**, *101*, 5368 – 5373.
[5] W. S. Knowles, *Angew. Chem.* **2002**, *114*, 2096 – 2107; *Angew. Chem. Int. Ed.* **2002**, *41*, 1998 – 2007.
[6] R. Noyori, *Angew. Chem.* **2002**, *114*, 2108 – 2123; *Angew. Chem. Int. Ed.* **2002**, *41*, 2008 – 2022.
[7] S. J. Zuend, M. P. Coughlin, M. P. Lalonde, E. N. Jacobsen, *Nature* **2009**, *461*, 968 – 970.
[8] H. Xu, S. J. Zuend, M. G. Woll, Y. Tao, E. N. Jacobsen, *Science* **2010**, *327*, 986 – 990.
[9] H. U. Blaser, E. Schmidt in *Asymmetric Catalysis on Industrial Scale* (Eds.: H. U. Blaser, E. Schmidt), Wiley-VCH, Weinheim, **2004**.
[10] a) *Handbook of Asymmetric Heterogeneous Catalysis* (Eds.: K. Ding, Y. Uozumi), Wiley-VCH, Weinheim, **2008**; b) Z. Wang, G. Chen, K. Ding, *Chem. Rev.* **2009**, *109*, 322 – 359.
[11] M. Heitbaum, F. Glorius, I. Escher, *Angew. Chem.* **2006**, *118*, 4850 – 4881; *Angew. Chem. Int. Ed.* **2006**, *45*, 4732 – 4762.
[12] J. M. Thomas, R. Raja, D. W. Lewis, *Angew. Chem.* **2005**, *117*, 6614 – 6641; *Angew. Chem. Int. Ed.* **2005**, *44*, 6456 – 6482.
[13] a) P. Herold, A. F. Indolese, M. Studer, H. P. Jalett, U. Siegrist, H. U. Blaser, *Tetrahedron* **2000**, *56*, 6497 – 6499; b) M. Studer, S. Burkhardt, A. F. Indolese, H. U. Blaser, *Chem. Commun.* **2000**, 1327 – 1328.
[14] H. U. Blaser, S. Burkhardt, H. J. Kirner, T. Mössner, M. Studer, *Synthesis* **2003**, 1679 – 1682.
[15] H. U. Blaser, B. Pugin, M. Studer in *Chiral Catalyst Immobilization and Recycling* (Eds: D. E. De Vos, I. F. J. Vankelecom, P. A. Jacobs), Wiley-VCH, Weinheim, **2000**, pp. 1 – 17.
[16] N. End, K. U. Schöning, *Top. Curr. Chem.* **2004**, *242*, 241 – 248.
[17] T. P. Yoon, E. N. Jacobsen, *Science* **2003**, *299*, 1691 – 1693.
[18] T. Mallat, E. Orglmeister, A. Baiker, *Chem. Rev.* **2007**, *107*, 4863 – 4890.
[19] C. Mondelli, A. Vargas, G. Santarossa, A. Baiker, *J. Phys. Chem. C* **2009**, *113*, 15246 – 15259.
[20] F. Hoxha, L. Königsmann, A. Vargas, D. Ferri, T. Mallat, and A. Baiker, *J. Am. Chem. Soc.* **2007**, *129*, 10582 – 10590.
[21] T. Bürgi, A. Baiker, *Acc. Chem. Res.* **2004**, *37*, 909 – 917.
[22] E. Tálas, J. L. Margitfalvi, O. Egyed, *J. Catal.* **2009**, *266*, 191 – 198.
[23] H. U. Blaser, M. Studer, *Acc. Chem. Res.* **2007**, *40*, 1348 – 1356.
[24] M. Studer, H. U. Blaser, C. Exner, *Adv. Synth. Catal.* **2003**, *345*, 45 – 65.
[25] H. U. Blaser, H. P. Jalett, W. Lottenbach, M. Studer, *J. Am. Chem. Soc.* **2000**, *122*, 12675 – 12682.
[26] R. Hess, T. Mallat, A. Baiker, *J. Catal.* **2003**, *218*, 453 – 456.
[27] M. Garland, H. U. Blaser, *J. Am. Chem. Soc.* **1990**, *112*, 7048 – 7050.
[28] G. A. Somorjai, Y. M. Li in *Introduction to Surface Science and Catalysis*, Wiley, New York, **1994**.
[29] G. A. Somorjai, J. Y. Park, *J. Chem. Phys.* **2008**, *128*, 182504 – 1/9.
[30] E. Schmidt, A. Vargas, T. Mallat, A. Baiker, *J. Am. Chem. Soc.* **2009**, *131*, 12358 – 12367.
[31] S. C. Tsang, Y. K. Chen, P. J. F. Harris, M. L. H. Green, *Nature* **1994**, *372*, 159 – 162.
[32] E. Dujardin, T. W. Ebbesen, H. Hiura, K. Tanigaki, *Science* **1994**, *265*, 1850 – 1852.

